Monitoring and control of wind-induced vibrations of hanger ropes of a suspension bridge

Xu G. Hua[*1], Zheng Q. Chen[1], Xu Lei[2], Qin Wen[1] and Hua W. Niu[1]

[1]*Key Laboratory for Wind and Bridge Engineering of Hunan Province, College of Civil Engineering, Hunan University, 410082 Changsha, China*
[2]*Power Research Science Institute of Guangdong Power Grid, 510000 Guangzhou, China*

Abstract. In August 2012, during the passage of the typhoon Haikui (1211), large amplitude vibrations were observed on long hangers of the Xihoumen suspension Bridge, which destroyed a few viscoelastic dampers originally installed to connect a pair of hanger ropes transversely. The purpose of this study is to identify the cause of vibration and to develop countermeasures against vibration. Field measurements have been conducted in order to correlate the wind and vibration characteristics of hangers. Furthermore, a replica aeroelastic model of prototype hangers consisting of four parallel ropes was used to study the aeroelastic behavior of hanger ropes and to examine the effect of the rigid spacers on vibration mitigation. It is shown that the downstream hanger rope experiences the most violent elliptical vibration for certain wind direction, and the vibration is mainly attributed to wake interference of parallel hanger ropes. Based on wind tunnel tests and field validation, it is confirmed that four rigid spacers placed vertically at equal intervals are sufficient to suppress the wake-induced vibrations. Since the deployment of spacers on hangers, server hanger vibrations and clash of hanger ropes are never observed.

Keywords: suspension bridge; hangers; wake-induced vibrations; vibration control

1. Introduction

The span length of suspension bridges has progressed significantly due to the advancement of design and construction technology. On the other hand, with increase of span length, wind-induced vibrations of hangers in suspension bridges have become a serious problem (Gimsing and Georgakis 2001). Large amplitude violent vibrations have been observed in long hangers of several well-known suspension bridges, including the Akashi Kaikyo Bridge in Japan (Saito *et al*. 2001), the Great Belt East Bridge in Denmark (Laursen *et al*. 2006), and the Xihoumen Bridge in China (Hua *et al*. 2015, Wen *et al*. 2018). Excessive wind-induced vibrations raise concerns about the fatigue problem at both ends of the hangers and can also cause visual discomfort for drivers.

Hangers are made of the conventional wire strand ropes or the relatively new parallel wire strands (PWS) with PolyEthylene sheath, and have circular or nearly circular cross-sections. From the view point of cost for construction and maintenance, hangers are commonly deployed in pairs or groups with close spacing. Due to the interference effects, the aerodynamic behaviors of closely spaced cylinders becomes very complex and is considerably different from that of a single isolated one, which is especially influenced by the arrangement of cylinders as well as the cylinder spacing (Blevins 1990, Wardlaw 1994,

Zdravkovich 1997, Zdravkovich 2003). According to the cylinders' position relative to the flow direction, the cylinder arrangement may be classified as the side-by-side, the tandem and the staggered arrangements. The interference effects of two cylinders will start when they are close to each other or when the rear cylinder is within the wake of the front one, covering a wide range of cylinder spacing. The former is called the proximity interference which encompasses all the three arrangements up to certain cylinder spacing of 1.5D ~6D (D is the cylinder diameter). The latter is referred to as the wake interference which extends as far as 20D downstream but is confined to the tandem and slightly staggered arrangements.

For vertical hanger pairs in suspension bridges, their spacing generally falls in the above interference regimes. The typical center-to-center (CC) spacing of hanger pairs in the Akashi Kaikyo Bridge is 9D, and the long hangers of 100 m~200 m are reported to suffer from violent vibrations with amplitudes up to 8D at wind velocity above 20m/s which is later verified as the wake-induced flutter of leeward hanger (Saito *et al*. 2001). For the Great Belt Bridge, the CC spacing of hanger pairs is about 5.5D~7.5D and large amplitude vibrations occurred more frequently at relatively low wind velocity range of 6~15 m/s (Laursen *et al*. 2006, Bitsch *et al*. 2010), but the exact mechanism seems to be not well understood (Gjelstrup *et al*. 2012). Park and Kang's experimental investigations showed that hanger ropes have superior aerodynamic stability than PWS hangers (Park and Kang 2008). Yagi *et al*. (2015) measured unsteady drag and lift aerodynamic forces on downstream circular cylinders and conducted 2-DOF flutter analysis to explain the driving mechanism of instability.

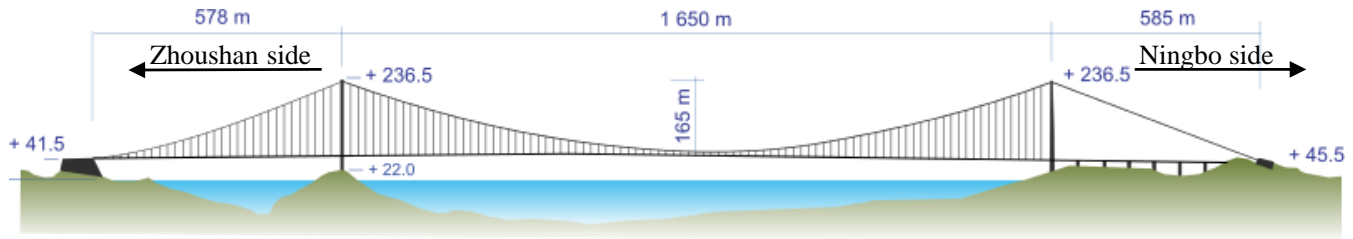∗Corresponding author, Professor
  E-mail: cexghua@hnu.edu.cn

Fig. 1 Layout of Xihoumen suspension Bridge (unit: m)

Countermeasures against wind-induced vibrations of hangers and stay cables are generally classified into three categories, namely aerodynamic treatments through surface indentation and winding helical wires, structural modifications through cross-ties and spacers, and damping enhancements by passive viscous dampers and mass dampers (Chen *et al*. 2004, Wang *et al*. 2005, Duan *et al*. 2006, Caetano 2007, Lu *et al*. 2017, Wang *et al*. 2018, Duan *et al*. 2019a, b) or semi-active MR dampers (Duan *et al*. 2005, Or *et al*. 2008, Duan *et al*. 2018). For suspension bridge hangers, spacers are generally incorporated to tie together hanger pairs at selected locations during design stage, like those used in bundled electrical conductors. Stockbridge-type dampers are occasionally adopted to mitigate the vortex-induced vibration of hangers in several suspension bridges including Severn Bridge, Humber Bridge, Bosprous Bridge, and Ulsan Bridge (Cigada *et al*. 1997, Jung *et al*. 2016). Saito *et al*. (2001) verified that the use of helical wires successfully suppressed the hanger vibrations in the Akashi-Kaikyo Bridge. However, Laursen *et al*. (2006) reported that the hanger spacers and helical wires were insufficient to inhibit the hanger vibrations in the Great Belt suspension Bridge, with vibration amplitudes reaching 2 m, and the vibration problem has not completely resolved yet (Hansen 2015). Therefore criterion for selection of suitable countermeasures against hanger vibrations is still rather crude and should be determined on a case-by-case basis.

The Xihoumen suspension bridge is a steel box-girder suspension bridge. It has a main span of 1650 m and a side span of 578 m with a suspended length up to 2228 m. In 2012, during the passage of the typhoon Haikui (1211), large amplitude vibrations were observed on a few long hangers, which destroyed some of viscoelastic dampers initially installed on hangers as countermeasures against the vortex-induced vibration. This incident called for special attentions from bridge owners. In this study, field and wind tunnel investigations were carried out in an attempt to identify the cause of vibration as well as to develop solutions. Wind and vibration characteristics of hangers measured from a temporary monitoring system are analyzed and correlated. The prototype hanger with most sever vibration is selected for wind tunnel study. Rigid spacers tying together hanger ropes are considered as vibration mitigation scheme and the minimum number of spacers required is evaluated by wind tunnel tests. The efficiency of spacers is further verified through field measurements on two identical hangers with and without spacers.

2. Observation on hanger vibrations in Xihoumen Bridge

2.1 Description of the Xihoumen Bridge

As an outstanding part of the Zhoushan Mainland-Islands Link, the Xihoumen Bridge is a two-span suspension bridge and carries four-lane roadway by twin steel box girders (Wang 2009). The bridge has a main span of 1650 m and a side span of 578 m with a total suspended length of bridge deck up to 2228 m, as shown in Fig. 1. The sag-to-span ratio of the bridge is 1/10. The bridge was open to traffic in 2010.

The bridge has a total of 238 hanger unit which vary in length from 2.5 m at mid-span to 169 m adjacent to main towers. Each hanger unit is formed by a set of two bare wire strand ropes working in double part. This means that each rope is looped over the main cable with both ends pin anchored at steel sockets which join the two ropes to form a single hanger. Fig. 2 illustrates the layout of the two ropes with four rope segments for a single hanger unit. At the main cable the wire ropes pass over grooves in cast steel cable bands, which are held in place on the main cable by friction induced by high tensile bolts.

The wire ropes for 8 sets of hangers closest to the pylon have a nominal diameter of 88 mm, those for the remaining hangers 60 mm. The CC spacing of the two ropes of a single hanger is 300 mm and 600 mm in the longitudinal and transverse directions of the bridge, respectively.
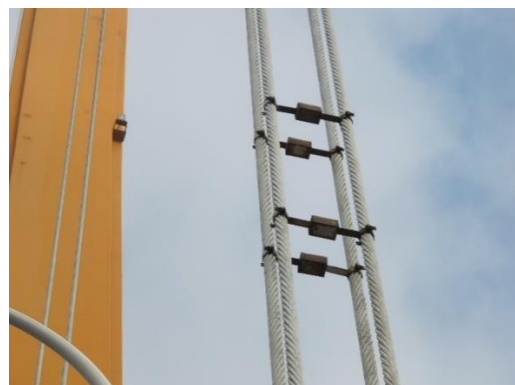

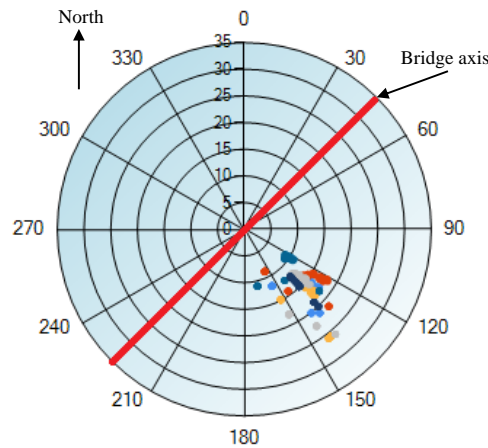Fig. 2 Layout of two wire ropes with four segments for a hanger pair

Fig. 3 Wind rose diagram at bridge site during typhoon Haikui (1211)

(a) longitudinal acceleration of hanger No. 28   (b) wind velocity at deck level
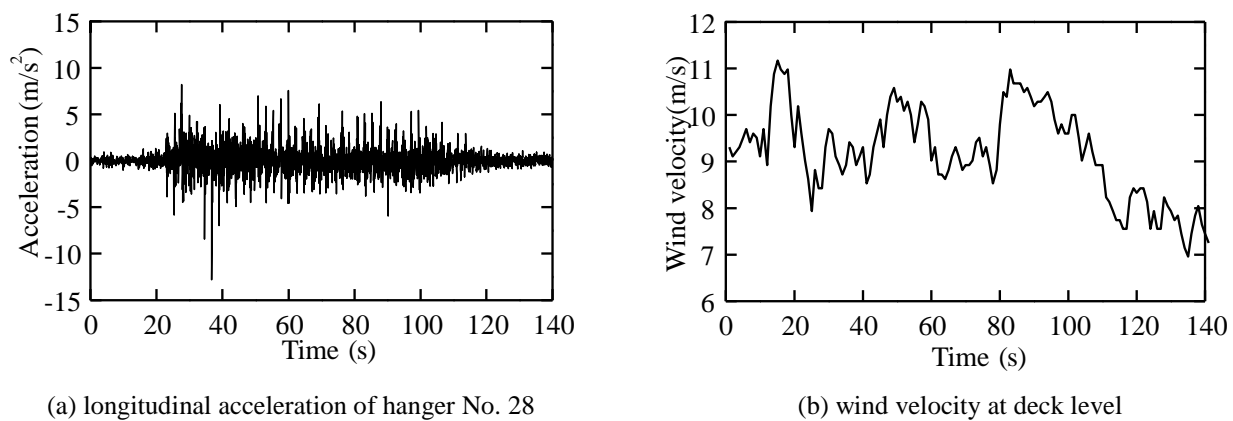
Fig. 4 Selected monitoring data

While they are closely spaced, hanger ropes were judged aerodynamically stable based on the past experiences. Rigid spacers holding apart the four ropes are not used. Instead, a connecting type viscoelastic damper is installed on pair of hanger ropes transversely in order to suppress vortex induced vibrations, as show in Fig. 2.

2.2 Monitoring of hanger vibrations

On 6-8 August 2012, the Typhoon Haikui (1211) hit the bridge in a direction nearly perpendicular to the bridge axis. According to the measurement data recorded by anemometers at deck level, the maximum 10min mean velocity is about 23 m/s, and the maximum 3s gust is about 31 m/s (HCCL 2012). Fig. 3 showed the wind rose diagram measured at bridge site during typhoon Haikui (1211). Large amplitude vibrations were observed on longer hangers at either side of bridge pylon, and the maximum accelerations recorded at hangers' mid-span reaches to 2.06g. As only one accelerator in the transverse direction is installed per hanger, the detailed vibration characteristics of the hanger ropes are not available. Based on the video shooting, the vibration orbits of the two wire ropes (four segments as shown in Fig. 2) are very complicated,

including the in-phase vibrations and the out-of-phase vibrations of two ropes, and vary with wind velocity and wind direction. This observation is different from those in hangers of the Akashi-Kaikyo Bridge where only the leeward cable displayed excessive vibrations. Additionally, the hanger responses built up rapidly just in a few seconds. The violent vibrations caused clash of strand ropes and also destroyed the viscoelastic dampers already installed. It was later become apparent that the dampers have no effect on vibration mitigation in the longitudinal direction of the bridge. Even in the transverse direction, the dampers take effects only for out-of-phase vibrations of two hanger ropes. The hangers used in the Xihoumen Bridge are the bare wire strand ropes, which are different from those in the Akashi-Kaikyo Bridge and Great Belt East Bridge.

A monitoring system for bridge hangers is set up to study the vibration characteristics and the occurring conditions of the vibration. The second longest hangers, denoted as No. 2 at side span and No. 28 at main span, are selected for monitoring, as they have the most violent vibrations. The system has comprised 2 anemometers mounted 8m above deck level and 19 accelerometers for monitoring the vibrations of hangers, main cables and bridge deck. The wind direction measured from the

Table 1 Parameters for hanger unit No. 28

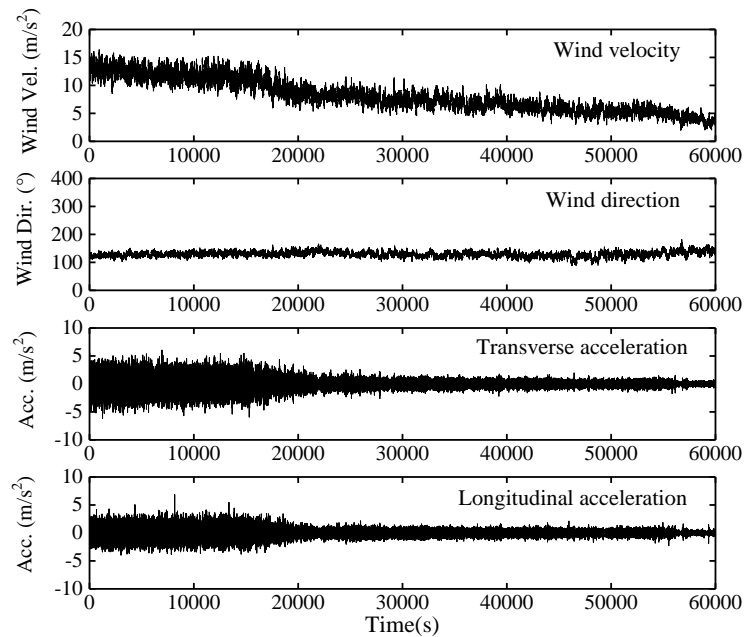| Length (m)	Tensile Force (kN)	Sectional Area (mm^2)	Density (kg/m^3)	Modulus of Elasticity (N/m^2)
160.6	495.8×4	3960×4	8000	$1.1×10^{11}$

Fig. 5 Selected data of acceleration and wind velocity for hanger No. 28

anemometers is calibrated as 0° when wind blows from south. Each hanger is instrumented with 8 accelerometers at a height of 15 m above deck level, measuring longitudinal and transverse accelerations of hangers. The transverse acceleration of main cables and vertical acceleration of bridge deck near hanger ends are also monitored to study effect of support excitations.

Fig. 4 shows the longitudinal acceleration data of one of wire ropes of hanger No. 28, as well as the corresponding wind velocity at deck level. Note that the fundamental natural frequency of the hanger is 0.42 Hz, and a natural period 2.25s. As seen in the Fig. 4(a), at the very beginning the vibration is small with acceleration amplitude as low as 1.0 m/s^2, which is caused by vortex-induced vibrations of higher modes of the hanger. When wind velocity increases over about 10 m/s, the acceleration builds up rapidly just in about 10 seconds and clash of hanger ropes takes place.

Upon clash the time interval of two adjacent predominant peaks of acceleration is about 2.3s which is quite close to the fundamental period of the hanger, implying that the vibration is dominated by the first mode of the hanger. Fig. 5 shows another example of measurement data of acceleration and wind velocity for the hanger No. 28.The wind direction is about 130° which is nearly perpendicular to bridge axis. The accelerations in both directions are of the same magnitude. Furthermore, it can be seen that the large amplitude vibrations disappear when wind velocity reduces below approximately 10 m/s.

3. Wind tunnel tests

3.1 Prototype hanger

In order to investigate the causes and occurring condition of large amplitude vibration as well as to find countermeasures against vibration, wind tunnel tests are performed by using aeroelastic models. The hanger unit No. 28 is selected as prototype for wind tunnel tests. Table 1 shows the structural parameters for the prototype hanger. Fig. 6 shows the cross-section of wire strand rope, which consists of a central core strand surrounded by 8 strands with the same pitch and direction of helix. The helix angle for the strand ropes is 30°.

According to the ambient vibration data collected, the natural frequencies and damping ratios for the first 5 modes of the hanger are identified by using the stochastic subspace identification (SSI) method. Table 2 listed the natural frequencies and damping ratios identified from ambient data. It can be seen that the fundamental natural frequency is 0.42 Hz, which is less than those in the Akashi-Kaikyo Bridge (0.48 Hz) and the Great Belt East Bridge (0.64 Hz). Due to the obvious hysteretic effects, the damping ratios for strand ropes are expected to larger than those for PWS hangers whose damping ratios may be as low as 0.05%.

3.2 Aeroelastic model of hangers

Wind tunnel tests are carried out in the HD-2 wind tunnel at the Hunan University. It has three test sections.

Table 2Measured modal properties for the first 5 modes of the hanger

Model shape	Modal frequency (Hz)	Damping ratio (%)
	0.42	0.44
	0.85	0.30
	1.27	0.33
	1.70	0.43
	2.12	0.37

Table 3 Properties of the prototype hanger and its aeroelastic model

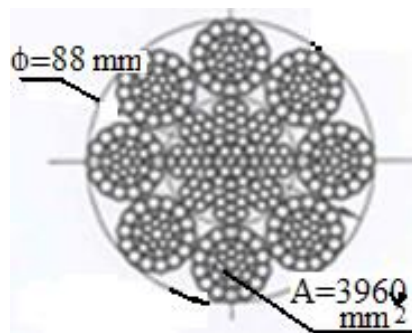| Parameter name	Prototype	Scaling ratio	Model
Length (m)	160	λ_L =1:36	4.44
Diameter (m)	0.088	λ_L =1:36	0.0025
Longitudinal spacing (m)	0.6	λ_L =1:36	0.016
Transverse spacing (m)	0.3	λ_L =1:36	0.008
Mass per unit length (kg/m)	31.7	λ_m =1:36^2	0.024
Wind speed (m/s)	--	λ_U =1:2.44	--
Bending frequency (Hz)	0.42	λ_f =15:1	6.20
Damping ratio (%)	0.4 ~ 0.5	λ_ζ =1:1	0.3
Displacement(m)	--	λ_L=1:36	--
Acceleration (m/s^2)	--	λ_a =15^2:36	--

Fig. 6 Cross-section of the wire rope of the hanger No. 28

The test section used for the present study is 4.5 m high and 5.5 m wide. The maximum wind speed is about 15 m/s, and all of the test cases were carried out in a turbulent flow with turbulent intensity of 5.0%~8.0%.

A geometric scale ratio λ_L of 1:36 is selected for design of aeroelastic model of the prototype hanger. Careful design of the full aeroelastic model is performed to satisfy the similarity requirements both in the mass and geometry. Steel wire with a diameter of 0.95 mm and a length of 4.44 m was used as the central core of the aeroelastic model, and 2 copper wires and 6 aluminum wires are winding around the steel wire central core in a helical angle of 30° which is same as the prototype hanger. By this way, both the mass and geometric similarities are fulfilled without imposingadditional mass or coating on the model. The longitudinal and transverse spacing of the four ropes of the

model are the same those in the actual bridge hanger. The four model ropes are clamped at both ends and their tensile forces can be easily adjusted. Fig. 7 shows the overview and detailed geometry of the full aeroelastic model in wind tunnel.

In addition to the geometric similarity, the aeroelastic modeling of structures generally requires equality of a few non-dimensional quantities, which includes the Froude number, Cauchy number, density ratio, and Reynolds number. Froude number scaling which maintain the correct balance between flow inertia and gravity force is insignificant in this case and not followed. This allows for the free choice of velocity scaling between model and prototype. The velocity scaling λ_U is set as 1:2.44. The scaling of modal frequency λ_f is determined as 15:1. The structural characteristics of the prototype hanger and the

Fig. 7 Full aeroelastic model of parallel hangers in wind tunnel

0.2 gram. The measured acceleration at the instrumented points can be converted to the maximum response of a particular mode simply by multiplyinga mode shape factor for that mode.

3.3 Vibration characteristics of aeroelastic model

The aeroelastic model is exposed to increasing wind velocity of 0~13 m/s in wind tunnel. Experiment results indicate that the downstream strands start to vibrate in an elliptic orbit when the wind velocity reaches a certain thresholds of about at model-scale velocity of 5.5 m/s, as will be shown later. The vibration becomes larger with increase of wind velocity. At larger wind velocity, the four strands come into substantial vibrations and finally clash, the vibrations become irregular. The most sever hanger vibration happens for wind incidence angle of 15°. Therefore the selected results at wind incidence angle of 15° will be presented in the following. The accelerations of model hanger are given at instrumented locations and in model scale.
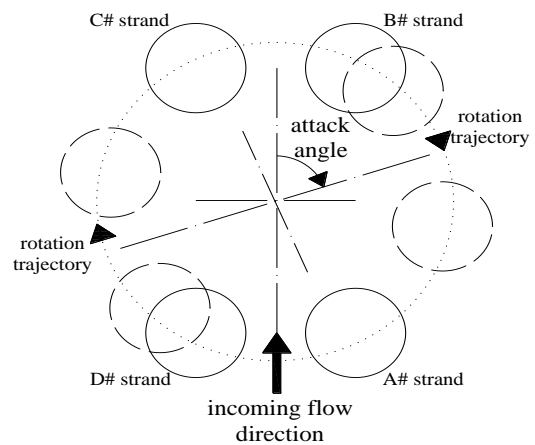

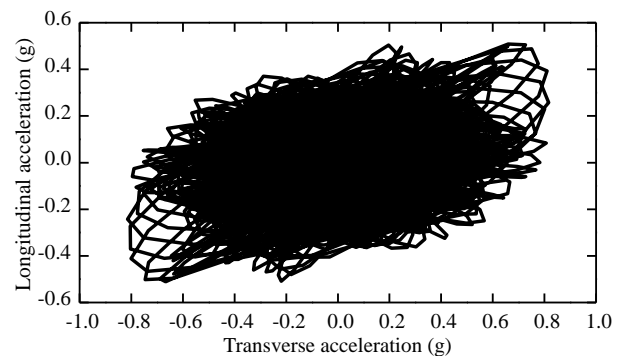Fig. 8 Definition of wind incidence angle

model are summarized in Table 3. The Scruton (Sc) number, which is defined as $m\zeta/\rho d^2$, is approximately 10.

The model-scale wind velocity in wind tunnel varies from 0 to 13 m/s, and the full-scale wind velocity is therefore 0~32 m/s according to velocity scaling. The definition of wind incidence angle is illustrated in Fig. 8. A total of 11 scenarios of wind attack angles are tested, covering 0°, 10°, 15°, 20°, 25°, 30°, 45°, 60°, 70°, 80° and 90°. A 0° wind attack angle means that the wind direction is perpendicular to bridge axis, while 90° wind attack angle parallel to the bridge axis.

The wind velocity in wind tunnel is measured with a TFI cobra probe positioned 0.5 m above the ground and 1.0 m ahead of the model. The accelerations of four model strands are monitored by 8 mini piezoelectric accelerators (Model LCO408T, Lance Technologies Inc.) at a height of 0.42 m above the ground, corresponding to a prototype value of 15 m. For each strand shown in Fig. 8, acceleration responses in the longitudinal and transverse directions of the bridge are measured. The weight of each accelerator is

Fig. 9 Orbit of model strands for the first mode at model velocity *U*=11.9 m/s

(a) accelerationresponse
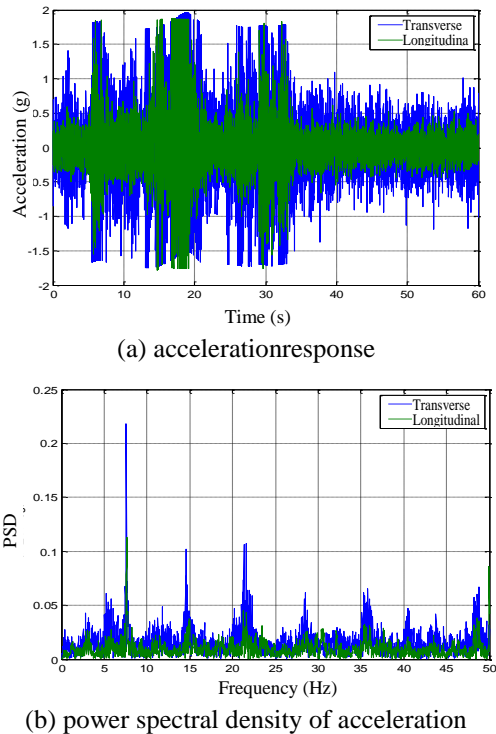

(b) power spectral density of acceleration

Fig. 10 Model strand response for model-scale velocity *U*=13 m/s
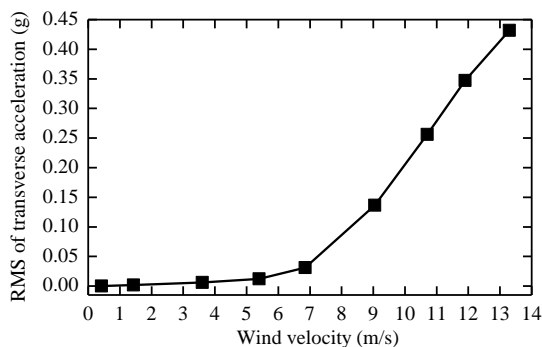

Fig. 11 Variation of transverse modal accelerations of model strand C

Fig. 9 illustrates the vibration trajectory of the model strands for the first mode at model-scale wind velocity of 11.9 m/s. It is seen the model strands vibrates in both directions of the bridge axis, and the vibration orbit is close to an oval with its longer axis in the bridge's transverse direction, which is close to the wind direction. The transverse acceleration is about 50% larger than those in longitudinal direction. The irregularity of the response is partially attributed to the turbulence in wind which reaches to about 5% for the test section used. Fig. 10 shows the longitudinal and transverse accelerations of the model strand at a wind velocity of 13 m/s, and their power spectral densities are also provided. It is indicated clearly that the fundamental mode of the model dominates the dynamic responses in both directions.

Fig. 11 shows the variation of transverse modal accelerations of model strand C with increasing wind velocities for the first mode. For wind velocities below about 5.5 m/s, the acceleration responses increase gradually. Once the critical velocity is reached, the acceleration responses build up rapidly with a power-law exponent of approximately 3.8, which suggests a kind of dynamic instabilities. The power-law exponent for the acceleration amplitude in the present study is a little smaller than those obtained from section model tests and aeroelastic model tests in smooth flow, where the power-law exponent usually exceeds 5 especially at low damping level (Tokoro *et al.* 2010, Takeguchi and Fukunaga 2012, Lee *et al.* 2013). For wind-induced buffeting due to atmospheric turbulence, the variation curves of amplitudes with wind velocity usually have a power-law exponent of 1.5~2.0. It may be concluded that the response is not caused by wind buffeting. Based on the wind tunnel tests, the full-scale critical wind velocity is about 13 m/s, and is larger than the field observation which may be caused by uncertainty in structural damping parameters.

As far as the Xihoumen Bridge is concerned, the ratios of center-to-center hanger spacing with respect to its diameter are 3.4 and 6.8 for the longitudinal and transverse directions of the bridge. It is apparent that both the proximity interference and wake galloping could occur for particular wind directions. Recall that the hanger consists of four strands for the Xihoumen Bridge. It implies that the
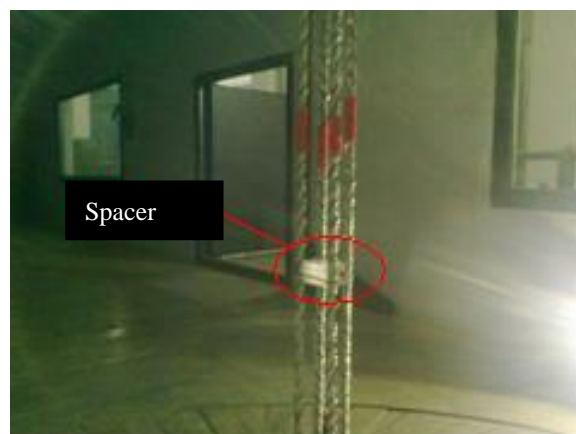

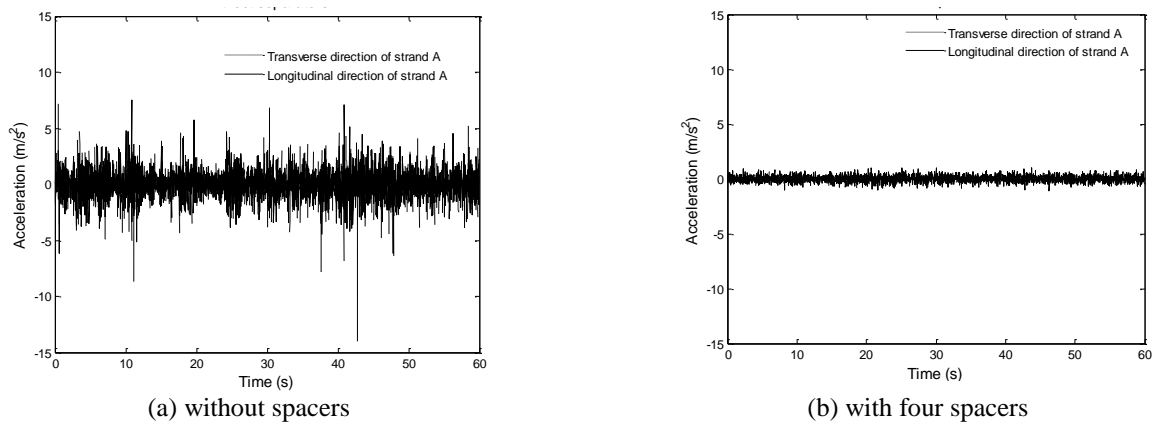Fig. 12 Spacer used to tie together four strands of the model

(a) without spacers   (b) with four spacers

Fig. 13 Acceleration of strand A of the model at model-scale velocity U=13 m/s
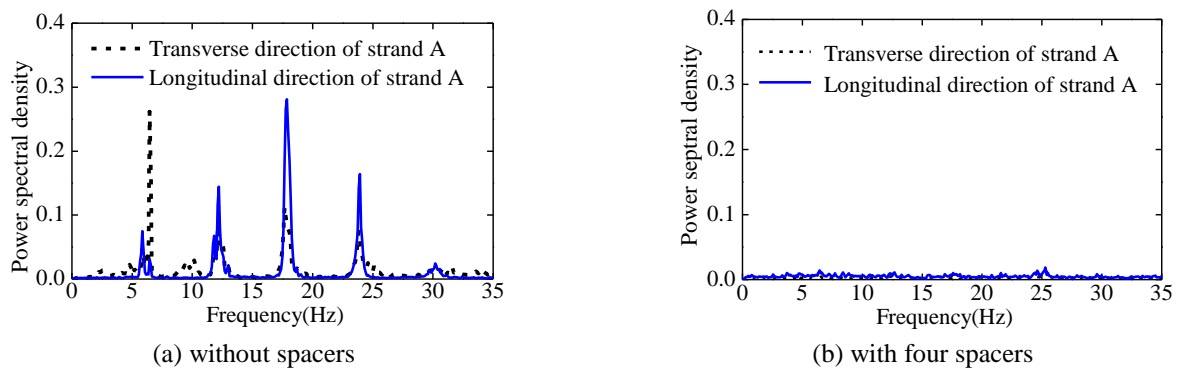

(a) without spacers   (b) with four spacers

Fig. 14 Power spectral density of acceleration of strandA at U=13 m/s

occurring conditions of large amplitude vibrations are much easier to satisfy for the hangers in the Xihoumen Bridge. Accordingly, the vibration characteristics are also much more complicated.

3.4 Vibration control scheme

Aerodynamic countermeasure by using helical wires is not considered since the wire strand ropes are already in helical shapes. As the viscoelastic dampers installed between hanger ropes were destroyed by the excessive vibrations, a first natural solution is to replace them with rigid spacers which interlock the four strands of a hanger at specified heights. It is well known that both the Scruton number and structural modal frequency play important roles on wind-induced vibration of flexible structures. Increase of the Sc number and modal frequency will reduce the vibration amplitude or promote the critical wind velocity triggering large amplitude vibrations. In this regard, the spacer effects on hanger vibrations can be explained twofold: (1) they increase the modal frequencies of hanger subspan between two adjacent spacers; and (2) they increase the apparent Scruton number by integrating the four strands as one. Fig. 12 illustrates the one of spacers that ties together the four strands of the aeroelastic model.

In the following, wind-induced responses of the model hanger with different spacer numbers are measured at varying wind velocities but fixed wind attack angle of 15°. Again, the measurement results are shown in the bridge-axis coordinate system and refer to model-scale values.

3.5 Spacer effects on hanger vibrations

Due to large amount of experimental data, only some selected results will be presented. Illustrated in Figs. 13(a) and 13(b) are the accelerations of the strand A of the model hanger without spacers and with four spacers, respectively, at a model-scale velocity of 13 m/s. It can be seen that the accelerations in longitudinal and transverse directions are significantly reduced for the model with four spacers, and clashing of model strands is not observed. Fig. 14 shows the corresponding power spectral density of acceleration responses. Without spacers, there are obvious peaks at modal frequencies of the lower-order modes, which may cause strands to clash.

After incorporating four spacers, no obvious peak at the first five modes of the model is observed, demonstrating that the vibrations of the model strand A in Fig. 13(b) are caused by higher-order modes.
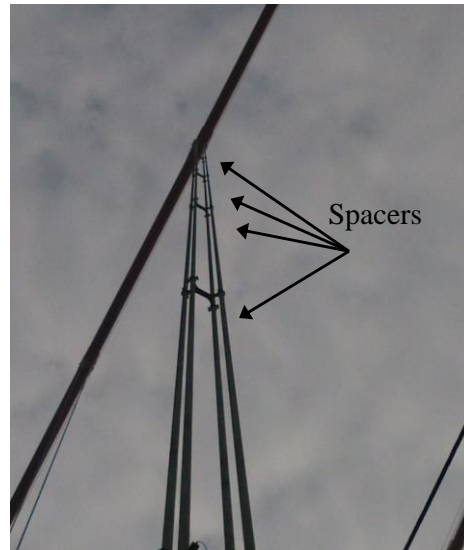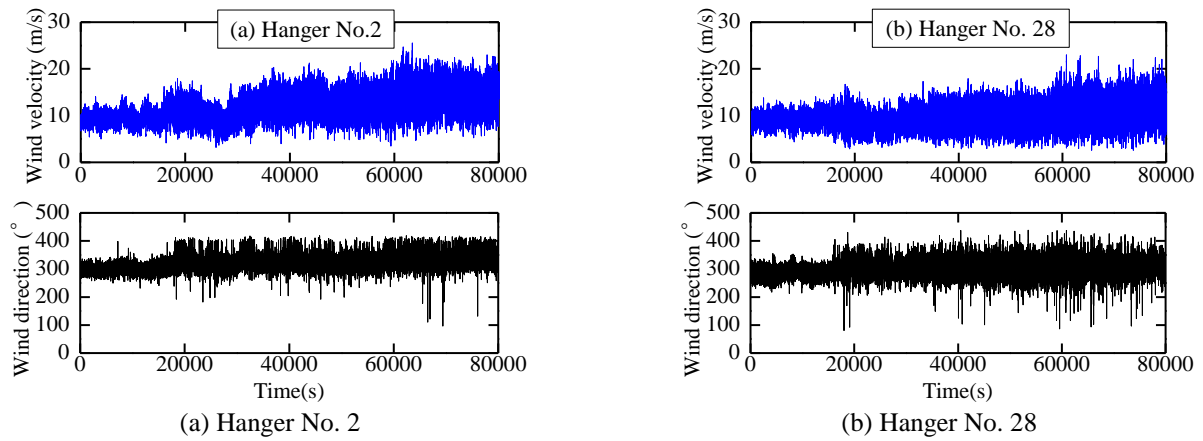
Fig. 15 Four sets of spacers on hanger No. 28

(a) Hanger No. 2

(b) Hanger No. 28

Fig. 16 Wind characteristics on 24 July 2014
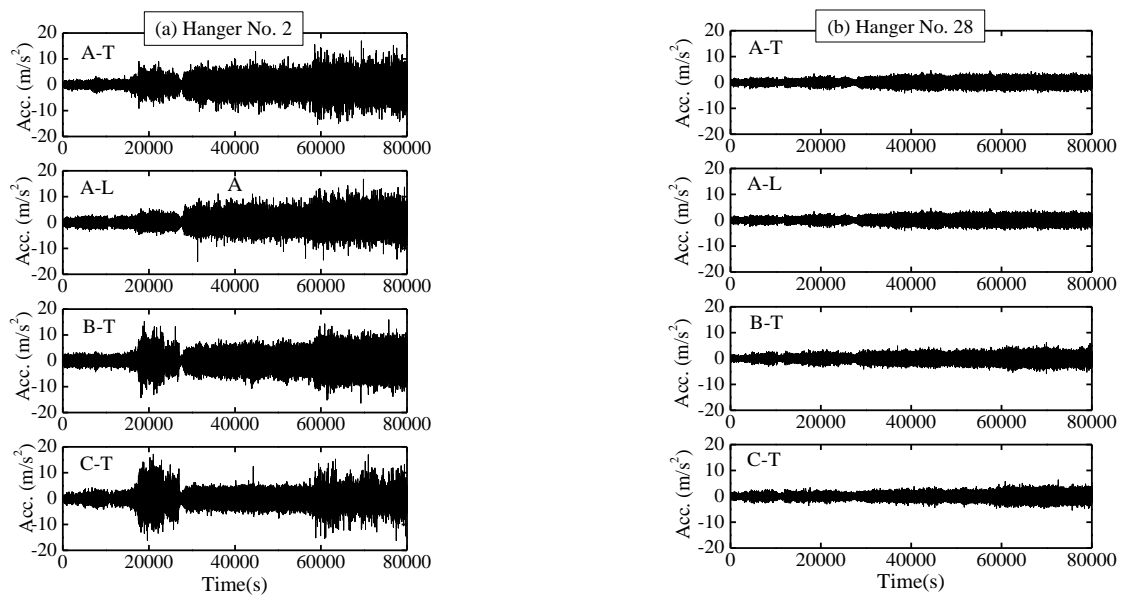
Fig. 17 Accelerations measured on hanger No. 2 and No. 28 on 24 July 2014

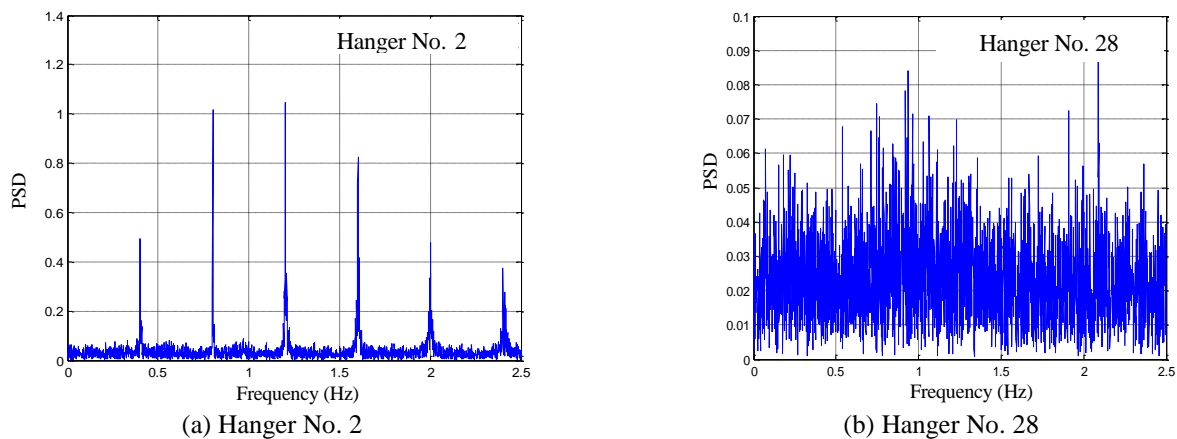(a) Hanger No. 2   (b) Hanger No. 28

Fig.18 Power spectral density of hanger accelerations

4. Field validation

According to wind tunnel experiments, a total of four sets of spacers were installed on hanger No. 28, each of them interlocking the strand ropes of a hanger at particular height. Fig. 15 shows the hanger with four spacers. Hanger No. 2, which has the same structural parameters as hanger No. 28, is left unattended for reference to evaluate the actual control performance.

Measurement data of wind direction and wind velocity on July 24 2014 are shown in Fig. 16. The mean wind direction relative to bridge axis is about 10°. Fig. 17 compares the longitudinal and transverse accelerations measured on hanger No. 2 and No. 28, respectively. Fig. 18 shows the power spectral density (PSD) of acceleration responses for selected strands on hanger No. 2 and hanger No. 28. After installing spacers, no resonance components are found for the first five modes. It is obvious that the acceleration responses of hangers have been significantly mitigated by installing spacers. Furthermore, one may deduce that the exciting mechanism of large amplitude vibration of hangers is not associated with support excitations.

The measured data are band filtered to extract modal responses corresponding to the first five modes. The 1min-duration root-mean-squares (RMS) of modal responses for selected downstream strands are obtained and shown in Fig. 19 for hanger No. 2 and No. 28. It is shown that the vibration responses of the hanger No. 28 are significantly smaller than those of the hanger No. 2 for the first five modes. The modal acceleration vibration responses for the first five modes have been reduced approximately more than 60%. Based on the measured modal acceleration for the 5th mode, the modal displacement of hanger with spacers at measurement location (15 m above deck level) is about 0.55 cm, and the corresponding peak modal displacement is 0.60cm by multiplying the modal shape factor for the 5th mode.

5. Conclusions

In this study, field and wind tunnel experiments were carried out to identify the causes of large-amplitude hanger vibrations in the Xihoumen Bridge, and to develop potential solutions for the vibration as well. The main results are summarized as follows: (i) large amplitude hanger vibrations and clash of hanger ropes are observed on the bridge at wind velocities higher than 10 m/s and are dominated by the fundamental mode; (ii) wind tunnel tests by means of an aeroelastic model successfully reproduced the large amplitude hanger vibration and the most violent vibrations take place at a wind incidence angle of 15° relative to bridge transverse direction. The vibration is considered to be mainly attributed to wake interaction of hanger ropes; (iii) the full-scale critical wind velocity triggering large amplitude vibration of hangers retrofitted with four rigid spacers exceeds 32 m/s based on wind tunnel experiments; (iv) the dynamic response of the hanger with four rigid spacers are significantly reduced when compared to the reference hanger without spacers. Since the implementation of spacers on hangers, server hanger vibrations and clash of hanger ropes are never observed.

Acknowledgments

References

Bitsch, N., Jensen, J.L. and Andersen, J.E. (2010), "Fatigue monitoring system –Great Belt Bridge", *Proceedings of Bridge Maintenance, Safety, Management and Life-Cycle Optimization*, (Eds., Frangopol, D.M., Sause, R. and Kusko, C.), 341-346, CRC Press.

Blevins, R.D. (1990), *Flow-Induced Vibrations*, Van Nostrand Reinhold, New York, NY, USA.

Caetano, E. (2007), *Cable Vibrations in Cable-Stayed Bridges*,

IABSE, SED 9 edition, International Association for Bridge and Structural Engineering, Switzerland.

Chen, Z.Q., Wang, X.Y., Ko, J.M., Ni, Y.Q., Spencer, B.F., Jr., Yang, G. and Hu, J.H. (2004), "MR damping system for mitigating wind-rain induced vibration on Dongting Lake Cable-Stayed Bridge", *Wind Struct.*, **7**(5), 293-304. http://dx.doi.org/10.12989/was.2004.7.5.293.

Cigada, A., Diana, G., Falco, M., Fossati, F. and Manenti, A. (1997), "Vortex shedding and wake-induced vibrations in single and bundle cables", *J, Wind Eng. Ind. Aerod.*, **72**, 253-263. https://doi.org/10.1016/S0167-6105(97)00247-X.

Duan, Y.F., Ni, Y.Q. and Ko, J.M. (2005), "State-derivative feedback control of cable vibration using semi-active MR dampers", *Comput. - Aided Civil Infrastruct. Eng.*, **20**(6), 431-449.

Duan, Y.F., Ni, Y.Q. and Ko, J.M. (2006), "Cable vibration control using Magneto-rheological (MR) dampers", *J. Intel. Mat. Syst. Str.*, **17**(4), 321-325. https://doi.org/10.1142/9789812702197_0121.

Duan, Y.F., Ni, Y.Q., Zhang, H.M., Spencer, B.F., Jr., and Ko, J.M. (2019a), "Design formulas for vibration control of taut cables using passive MR dampers", *Smart Struct. Syst.*, in press

Duan, Y.F., Ni, Y.Q., Zhang, H.M., Spencer, B.F. Jr. and Ko, J.M. (2019b), "Design formulas for vibration control of sagged cables using passive MR dampers", *Smart Struct. Syst.*, Accepted.

Duan, Y.F., Tao, J.J., Zhang, H.M., Wang, S.M. and Yun, C.B. (2018), "Real‐time hybrid simulation based on vector form intrinsic finite element and field programmable gate array", *Struct. Control Health Monit.*, e2277; https://doi.org/10.1002/stc.2277.

Gimsing, N.J. and Georgakis, C.T. (2011), *Cable Supported Bridges: Concept and Design*, Wiley, New York.

Gjelstrup, H., Georgakis, C.T. and Larsen, A. (2012), "An evaluation of iced bridge hanger vibrations through wind tunnel testing and quasi-steady theory", *Wind Struct.*, **15**(5), 385-407. http://dx.doi.org/10.12989/was.2012.15.5.385.

Hansen, D.E. (2015), Personal communication, 3rd November 2015.

Highways Consultants Co. Ltd (HCCL) (2012), *Wind-induced responses of the Xihoumen Bridge and Jintang Bridge based on structural monitoring systems*, Research report (in Chinese).

Hua, X.G., Chen, Z.Q. and Li, S.Y. (2015), "Field measurement and wind tunnel tests of large amplitude hanger vibration in a suspension bridge", *Proceedings of the 10th China-Japan-Korea International Workshop on Wind Engineering*, May 30-31, 2015, Busan, Korea

Jung, W.H., Bang, M.K., Kim, S.J. and Kim, H.K. (2016), "Mitigation effect of vortex-induced vibration of suspension bridge hangers with Stockbridge dampers", *Proceedings of the 2016 World Congress on Advances in Civil, Environmental, and Materials Research (ACEM 2016)*, 28-30 August 2016, Jeju, Korea.

Laursen, E., Bitsch, N. and Andersen, J.E. (2006), "Analysis and mitigation of large amplitude cable vibrations at the great belt east bridge", *IABSE Symposium Report*. International Association for Bridge and Structural Engineering, 2006, **91**(3), 64-71

Lee, S., Choi, U., Jeong, H., Kim, C. and Kwon, S. (2013), "Interference effects on bridge hangers", *Proceedings of the 8th Asia-Pacific Conference on Wind Engineering*, 10-14 December 2013, Chennai, India

Lu, L., Duan, Y.F, Spencer, B.F. Jr., Lu, X.L. and Zhou, Y. (2017), "Inertial mass damper for mitigating cable vibration", *Struct. Control Health Monit.*, **24**, e1986, doi: 10.1002/stc.1986.

Or, S.W., Duan, Y.F., Ni, Y.Q., Chen, Z.H. and Lam, K.H. (2008), "Development of Magnetorheological dampers with embedded piezoelectric force sensors for structural vibration control", *J. Intel. Mat. Syst. Str.*, **19**(11), 1327-1338. https://doi.org/10.1177/1045389X07085673.

Park, H.G. and Kang, S.J. (2008), "Aerodynamic stability assessment of PWS and CFRC hanger ropes for suspension bridge by experiments", *Korean Society of Hazard Mitigation*, **8**(6), 21-30.

Saito, Y., Okano, S., Takeguci, M. and Miyazaki, M. (2001), "Wake galloping of the circular tandem cylinders and examination of the damping countermeasures", *J. Struct. Eng. A JSCE*, **47**(3), 957-966. (In Japanese)

Takeguchi, M. and Fukunaga, S. (2012), "Aerodynamic stabilization for wake-induced vibration in parallel hanger ropes of the Akashi Kaikyo Bridge", *Wind Eng.*, JAWE, **37**(4), 300-306.

Tokoro, S., Homatsu, H., Nakasu, M., Mizuguchi, K. and Kasuga, A. (2010), "A study on wake-galloping employing full aeroelastic twin cable model", *J. Wind Eng. Ind. Aerod.*, **88**(2-3), 247-261. https://doi.org/10.1016/S0167-6105(00)00052-0.

Wang, C.J. (2009), "The Zhoushan Mainland-Island Linking Project consisting of five-sea crossing bridges", *IABSE Symposium Report*, 237-293

Wang, W.X., Hua, X.G., Wang, X.Y., Chen, Z.Q., and Song, G.B. (2018), "Numerical modelling and experimental study on a novel pounding tuned mass dampers", *J. Vib.Control*, **24**(17), 4023-4036. https://doi.org/10.1177/1077546317718714.

Wang, X.Y., Ni, Y.Q., Ko, J.M. and Chen, Z.Q. (2005), "Optimal design of viscous dampers for multi-mode vibration control of bridge cables", *Eng. Struct.*, **27**(5), 792-800. https://doi.org/10.1016/j.engstruct.2004.12.013.

Wardlaw, R.L. (1994), "Interference and approximate effects", *Proceedings of Wind-Excited Vibrations of Structures,* (Ed., Sockel, L.), 321-363, Springer-Verlag Wien GMBH.

Wen, Q., Hua, X.G., Chen, Z.Q. and Niu, H.W. (2018), "Experimental study of wake-induced instability of coupled parallel hanger ropes for suspension bridges", *Eng. Struct.*, **167**(15), 175-187. https://doi.org/10.1016/j.engstruct.2018.04.023.

Yagi, T., Arima, M., Ogawa, S., Kosugi, T., Zain, M.R. and Shirito, H. (2015), "Investigation on wake-induced instabilities of parallel circular cylinders based on unsteady aerodynamic forces", *Proceedings of the 14th International Conference on Wind Engineering*, 21-26 June, Porto Alegre, Brazil.

Zdravkovich, M.M. (1997), *Flow Around Circular Cylinders, vol. 1.Fundamentals*, Oxford University Press, Oxford.

Zdravkovich, M.M. (2003), *Flow Around Circular Cylinders, vol. 2. Applications*, Oxford University Press, Oxford.